

Flood Flows of the San Pedro River

Introduction

This chapter addresses surface water flows of the San Pedro River with an emphasis on flood flows. In terms of total volume, the storm runoff or flood flow component of streamflow is much larger than the baseflow. Although individual flood flows can be very large, they are sporadic, with up to several months or more between such flows, and thus provide only an intermittent source of water to the stream. I discuss temporal patterns of flood regimes, from intra-annual to decadal, as well as spatial patterns over the length of the river.

Seasonal Patterns and Variability

The surface water hydrology of the San Pedro River basin has a distinctly seasonal regime. It is characterized by moderate and relatively consistent monthly streamflow during the winter wet season (primarily December through March), low streamflow in the late spring and early summer dry season (April through June), and greater and more variable flow during the summer wet season (July through September) (fig. 1). This seasonal pattern results from the spatial and temporal interplay of latitudinally shifting winter storm tracks (Aldridge and Hales 1984), and influxes of moist air dur-

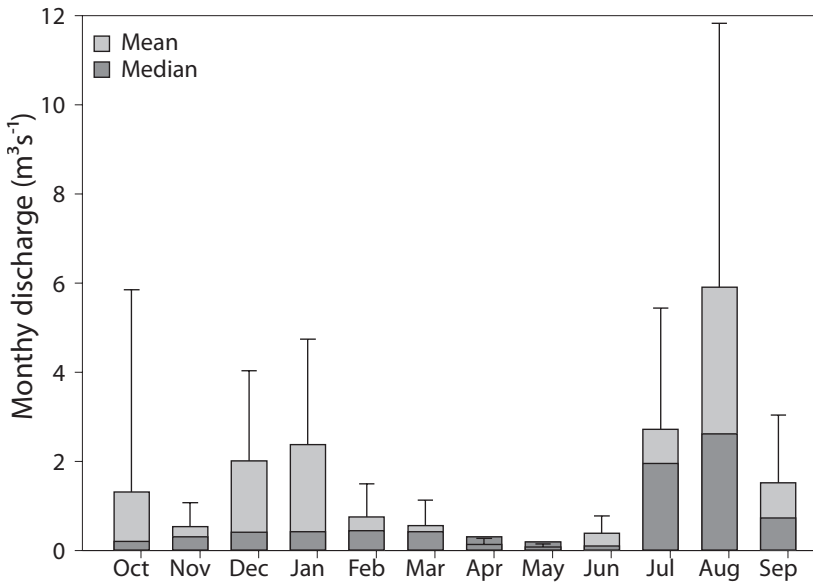


Fig. 16.1. Mean monthly streamflow variations for the San Pedro River at Charleston (#09471000), for 1943–2005. Values shown are the median and the mean plus one standard deviation.

ing the summer monsoon thunderstorm season (M. W. Douglas et al. 1993, Adams and Comrie 1997). In addition, the occasional penetration of tropical storm-related moisture during summer or fall (especially in September and October) can trigger copious runoff-producing rains (W. Smith 1986, Roeske et al. 1989).

Desert rivers throughout the world have highly variable flow regimes (Tooth and Nanson 2000, Bunn et al. 2006). The high variability of the San Pedro River, even within the seasonal framework, is evident in flow duration curves (fig. 2). While discharges are much larger during the summer months, they also tend to be more variable. The steep flow duration curve calculated for the warm season months implies high flow variability, while the flatter slope for the cooler months suggests that streamflow is being sustained more consistently by either surface runoff or groundwater. Flow duration curves calculated by decade show that while the low-flow portion of the curves has steepened dramatically over the past several decades, the high-flow portion has varied more idiosyncratically (fig. 3). For example, the curve for 1976–1985 is distinctly flatter than those for other decades. This decade experienced an exceptionally large tropical storm-related flood (October 1977) in addition to multiple occurrences of extreme winter flooding (December 1978, January 1979, December 1984).

Floods

Flood events contribute significantly to the overall surface water regime of the San Pedro, and thus the seasonality of annual flood peak occurrence mirrors the seasonal pattern of mean monthly flows (fig. 4a). The large differences between mean and median discharge for nearly all months (fig. 1)

Fig. 16.2. Flow duration curves (based on 1943–2005 water year mean monthly streamflow) for cool-season months, warm-season months, and all months combined, for the San Pedro River at Charleston.

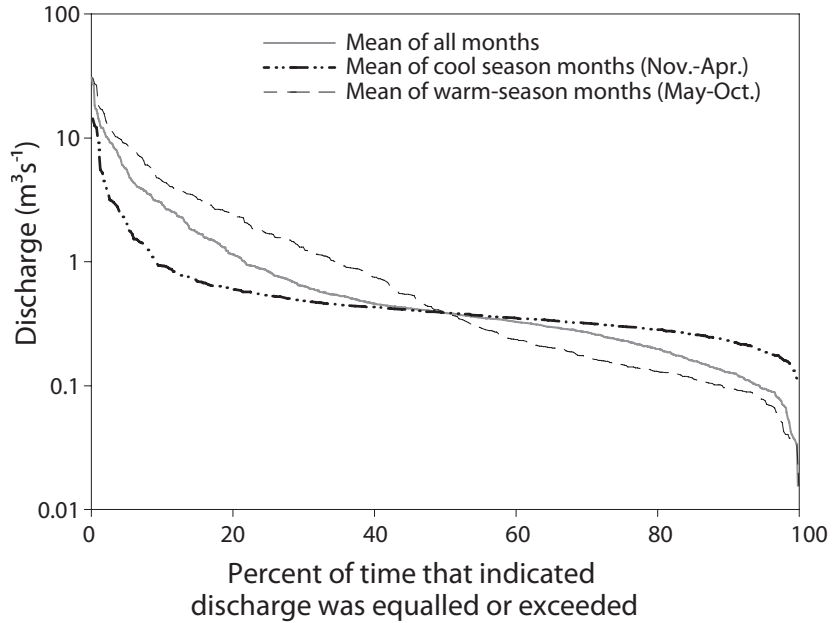
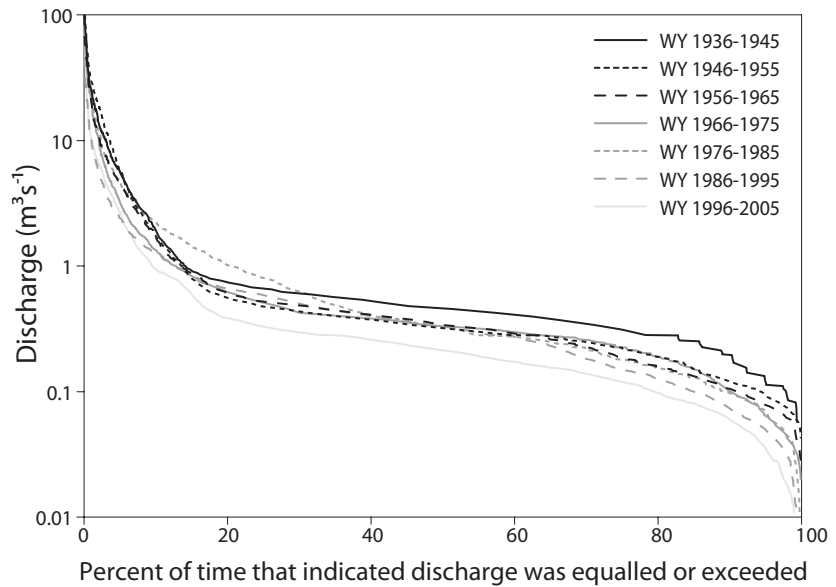


Fig. 16.3. Flow duration curves for seven decades of recorded daily mean streamflow of the San Pedro River at Charleston. Note: Prior to 1942, the Charleston gage was located at various positions along a six-mile reach of the river north of its present location, and thus the 1936–1945 decade may have included flow from the Babocomari River.



suggest that the flow from a relatively small number of extremely large events (floods) is an important component of the mean monthly discharge. Runoff-producing storms from three types of atmospheric patterns vary seasonally and interannually to control the frequency, magnitude, and timing of floods. Typically, the annual flow regime consists of a maximum peak in July or August, caused by intense summer convective rainfall, and one or more secondary winter flows in November through March, caused by synoptic storm precipitation (Hirschboeck 1991, House and Hirschboeck 1997).

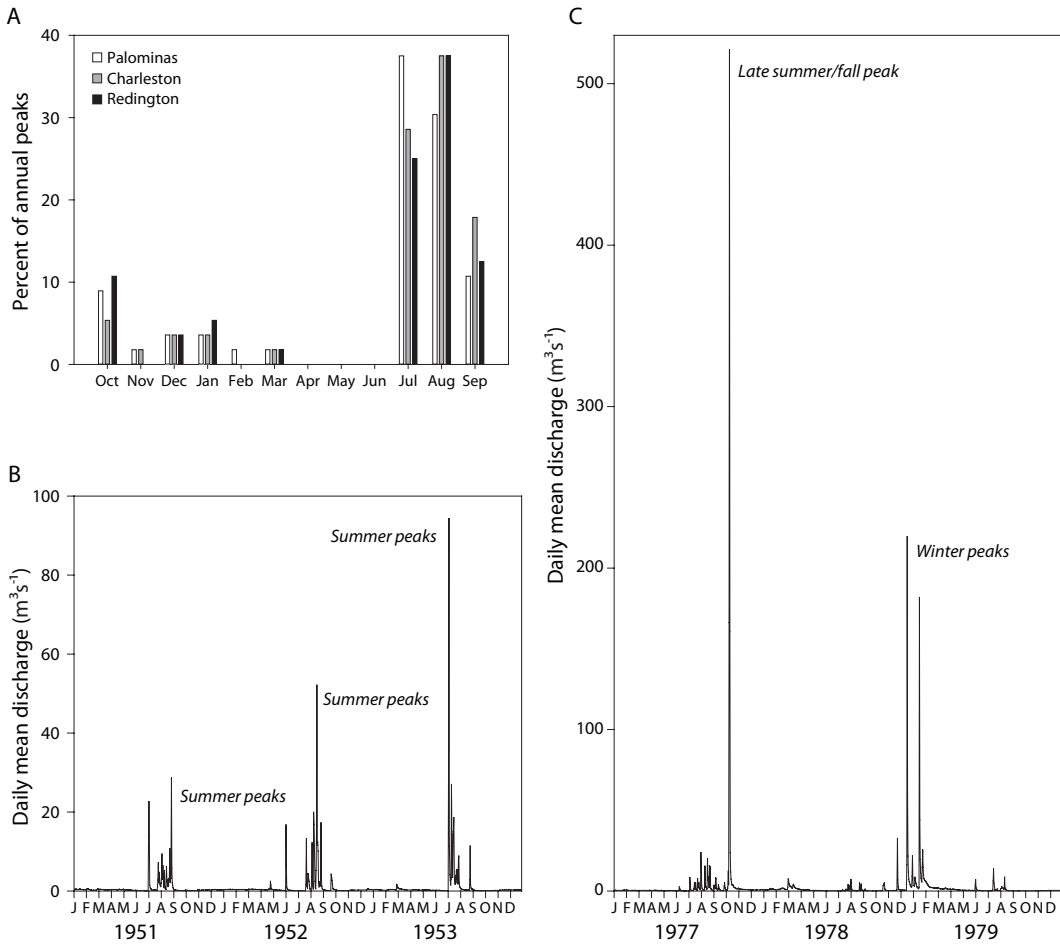


Fig. 16.4. Seasonal variations in San Pedro River flood peaks. (A) percent of annual floods occurring in each month at the Palominas, Charleston, and Redington gages for water years 1950 through 2005 (stations #9472000 and 9472050 combined for Redington), (B) three years of daily mean discharges at the Charleston gage during a period of dominance by summer flood peaks (maximum instantaneous peaks for the three years are $162 \text{ m}^3 \text{ s}^{-1}$ on 7-2-1951, $222 \text{ m}^3 \text{ s}^{-1}$ on 8-17-1952, and $243 \text{ m}^3 \text{ s}^{-1}$ on 7-7-1953), and (C) three years of daily mean discharges at the Charleston gage during a period of dominance by fall and winter flood peaks (maximum instantaneous peaks for the three years are $672 \text{ m}^3 \text{ s}^{-1}$ on 10-8-1977, $329 \text{ m}^3 \text{ s}^{-1}$ on 12-18-1978, and $334 \text{ m}^3 \text{ s}^{-1}$ on 1-8-1979).

SEASONAL FLOOD TYPES

Floods from convective storms. During 1950–2005, at the gaging stations of Palominas, Charleston, and Redington, almost 90 percent of the annual maximum flood peaks occurred during the months of July through October (fig. 4a). Two-thirds of the annual peaks occurred during July and August, the most active months of the summer monsoon thunderstorm season. Figure 4b illustrates the daily mean flow regime at the Charleston gage for three typical years during which summer flood peaks dominated. Several large peak-flow

events are evident in the daily discharge data, and instantaneous flood peaks on a given day can be two to five times greater than the daily mean value. The flashiness of the flow regime and the occurrence of multiple peaks are indicative of frequent and variable convective storm activity.

Floods from tropical storms. September and October typically are much dryer than July and August, although susceptibility to intense, tropical storm-related precipitation increases during these late summer/early fall months. Figure 4c illustrates one such event, the severe flood of October 1977 linked to rainfall from Tropical Storm Heather in the eastern Pacific Ocean, which caused widespread flooding throughout southern Arizona (Aldridge and Eychaner 1984).

Floods from synoptic winter storms. A flood season occurs in winter in response to less-intense but more-sustained precipitation events, which usually yield moderate discharges. Only 10 percent of the annual maximum flood peaks in the San Pedro River were recorded in the months of December through March during 1950–2005. When these winter floods do occur, however, they tend to be of longer duration than the more flashy summer flood peaks; hence, the total flow volume of a winter event may exceed that of a summer event, even though the summer flood has a larger instantaneous discharge peak. Occasionally, a sequence of winter storms can lead to an exceptionally active winter flood season, such as the sequence of peaks in the winter of 1978–1979 (fig. 4c). Since 1965 there has been an increase in the frequency of maximum annual flood peaks occurring in winter in the San Pedro basin.

TEMPORAL VARIABILITY

Extreme events. All of the extreme discharges of record for each of the gaging stations in the river basin have occurred during May through October. All are associated with convective storms or with convective rainfall enhanced by moisture from dissipating tropical storms (table 1). The extremes of record in tributaries with small drainage areas are more likely to be caused by convective storms in July or August, in contrast to the record floods on the main trunk stream where all but two are associated with late-season eastern Pacific tropical storms.

No single storm event stands out as the cause of the largest flood of record at *all* the gaging stations, in part because of different periods of record at each station. Two notable tropical storms, however, produced the largest flood of record at several stations. The flood associated with the unnamed tropical storm of September 1926 produced exceptionally large flood stages from Palominas in the upper basin to Redington in the lower basin. The gage at Charleston recorded the greatest discharge in the basin for this event, and it dominates the annual flood time series for this station (fig. 5), as well as that

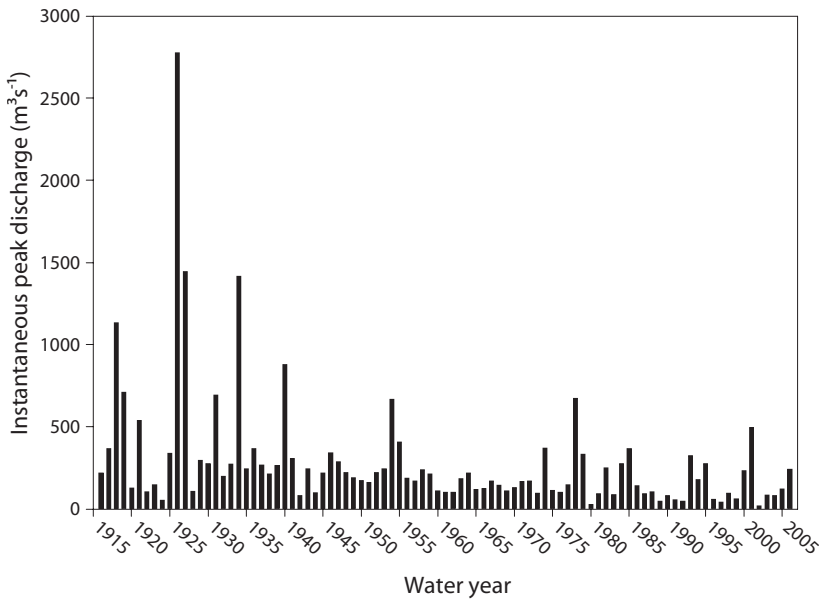


Figure 16.5. Annual flood peak time series of the San Pedro River at Charleston (values are instantaneous peak flows). The maximum recorded peak (September 1926) was $2,775 \text{ m}^3\text{s}^{-1}$.

of the Redington station downstream (not shown). Three gages in the lower basin experienced their greatest flood of record in response to intense precipitation linked to Tropical Storm Octave in October 1983 (water year 1984). This event also produced major flooding throughout central and southern Arizona, especially in the San Francisco, Gila, and Santa Cruz Rivers.

Intra-annual patterns. Limiting the discussion to only the largest floods in the record, or to the annual flood time series, neglects other peak flow events that play an important role in the flood hydroclimatology and riverine ecology of the basin. As suggested in daily mean discharge plots (figs. 4b, 4c), a given flow season in the San Pedro can be characterized by multiple flow events—some of substantial discharge—although only one will be recorded as the *annual* flood peak. Information on these lesser flood peaks can be obtained from a station's peaks-above-base record, which includes all discharges above a designated base discharge at a given recording station.

Figure 6 displays frequency histograms of the peaks-above-base record for the Charleston gage, separated by type of flood-causing storm for the period 1950–1985. The peaks were classified according to storm type based on a detailed analysis of weather charts and other sources (Hirschboeck 1987, 1988). (Histograms for the Palominas and Redington gages have patterns similar to that of the Charleston record.) This type of classification is more climatically accurate than a simple seasonal division of floods into winter, summer, and fall months (to represent synoptic, convective, and tropical storm-related floods, respectively) because some synoptic-scale circulation features (upper-level cutoff lows and short wave troughs) have contributed to enhanced flooding during the warm-season months, and some tropical storm-derived floods

TABLE 1. Maximum stage and discharge at San Pedro Basin stations for period of record.

Station number 0947-	USGS station name	Drainage area (km ²)	Period of record	Water year	Date	Storm type linked to flooding	Stage (m)	Peak discharge (m ³ s ⁻¹)	R.I. ³ (yrs)
0500	San Pedro at Palominas	1909	1926–05 ¹	1926	09/28/26	Tropical storm (TS)	7.3	—	—
1000	San Pedro at Charleston	3196	1916–05	1926	08/14/40	Tropical storm	5.0	623	20
1550	San Pedro near Tombstone	4481	1967–05	1978	09/28/26	Tropical storm	6.7	2,775	>100
1800	San Pedro near Benson	6449	1966–76	1972	10/09/77	TS Heather	3.5	685	50–100
2000	San Pedro near Redington	7581	1926–97	1972	08/26/72	Convective	3.2	278	<10
2050	San Pedro at Redington Bridge near Redington	8019	1999–05	1926	09/28/26	Tropical storm	6.6	2,549 ²	>100
3100	San Pedro below Aravaipa Creek near Mammoth	11248	1980–84	2003	07/22/03	Convective	4.6	167	—
3500	San Pedro at Winkelman	11533	1919–83 ¹	1984	10/01/83	TS Octave	5.4	3,823	>100
				1984	10/01/83 ²	TS Octave	—	3,823	>100

Main Channel

0900	San Pedro Tributary near Bisbee	13.6	1963-79	1965	09/04/65	TS Emily	3.7	41.3	—
1087	Walnut Gulch 63.111 near Tombstone	0.6	1962-81	1976	07/27/76	Convective	—	15.3	>100
1090	Walnut Gulch 63.009 near Tombstone	23.6	1967-81	1972	07/24/72	Convective	—	74.8	25-50
1110	Walnut Gulch 63.015 near Tombstone	23.9	1955-81	1971	08/10/71	Convective	—	35.4	10-25
1185	Walnut Gulch 63.103 near Tombstone	0.7	1963-81	1975	07/17/75	Convective	—	0.9	<10
1195	Walnut Gulch 63.007 near Tombstone	13.5	1966-81	1972	08/12/72	Convective	—	73.3	50-100
2100	Peck Canyon Tributary near Redington	20.8	1968-81	1972	08/12/72	Convective	2.8	123	>50
3000	Aravaipa Creek near Mammoth	1391	1919-94 ¹	1984	10/02/83	TS Octave	5.1	2,005	>100
3200	Green Lantern Wash near Winkelman	9.4	1964-76 ¹	1981	05/01/81	Convective	2.7	105	20-40

Tributaries

¹Observations for some years in record are missing.

²Discharge or date is estimated.

³R.I. = Recurrence Interval (R.I. estimates based on Perry et al. 2001).

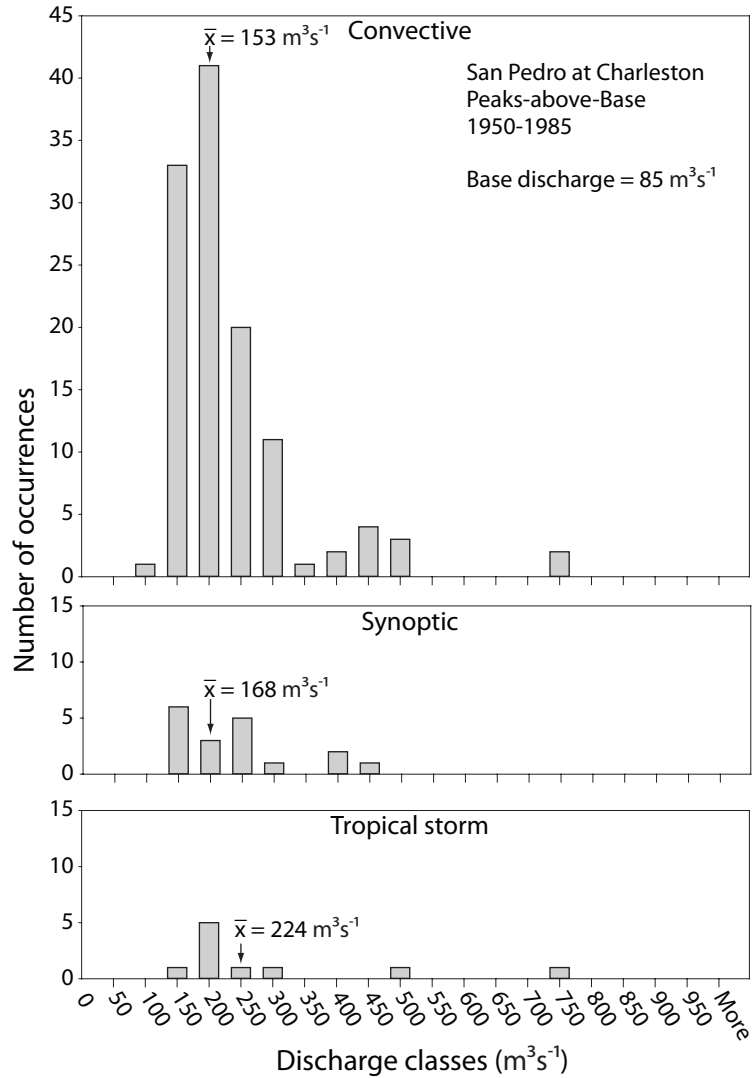


Figure 16.6. Histograms of instantaneous peaks-above-base discharge for convective, synoptic, and tropical storm floods recorded at the Charleston gage (1950-1985).

have occurred in July and August, even though the tropical storm influence is most pronounced in September and October in southern Arizona.

The flood-type classification shows the dominance of frequent summer peaks that are produced by intense convective rainfall events, but also emphasizes that most of these floods have moderate peak discharges (mean = $153 \text{ m}^3\text{s}^{-1}$), whereas the smaller populations of floods having synoptic or tropical storm influences have larger mean discharges ($168 \text{ m}^3\text{s}^{-1}$ for synoptic storms, $224 \text{ m}^3\text{s}^{-1}$ for tropical storms). Hence, a shift to a climatic regime favoring more frequent synoptic or tropical storms could alter the magnitude and frequency of flooding in the San Pedro basin.

Decadal patterns. Figure 7, which shows the Charleston annual flood record classified by flood type, illustrates that abrupt shifts in flood type have occurred in the San Pedro basin over the twentieth century. This is seen most

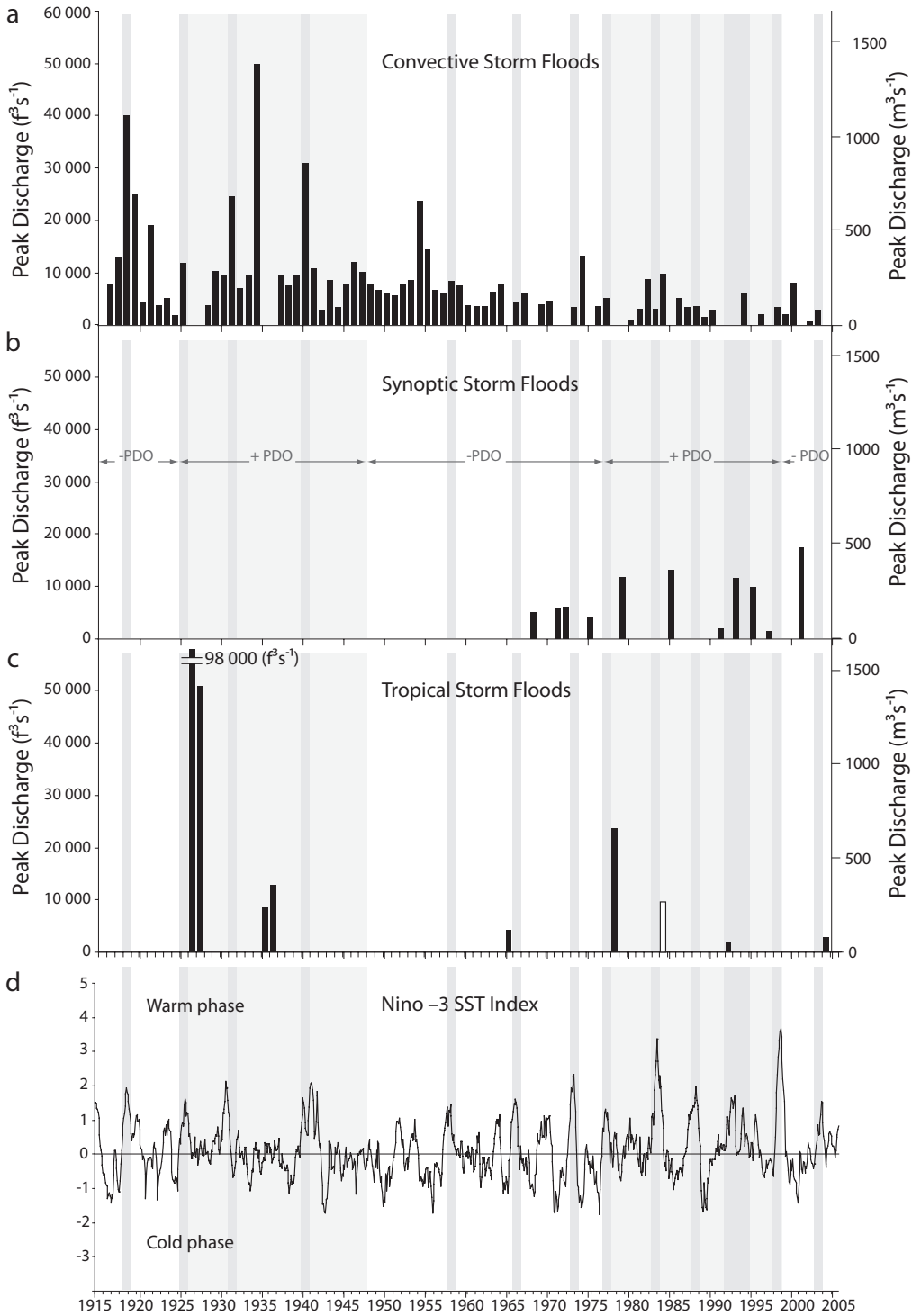


Fig. 16.7. Annual flood time series of the San Pedro River at Charleston, classified by flood-producing storm type: (a) convective, (b) synoptic, and (c) tropical, plotted with (d) the Niño-3 SST Index. Also shown are El Niño years (gray vertical lines) and positive (+) (shaded) and negative (-) phases of the PDO. (Flood values are instantaneous peak flows. An open bar is plotted for the October 1983 tropical storm flood which was the annual flood at downstream gages, but not at Charleston.)

dramatically after 1965 when there was a shift for annual floods to be produced more frequently by synoptic and tropical storms and less frequently by convective storms. During the post-1965 period, the magnitudes of nearly all synoptic storm floods exceeded that of the summer convective annual floods. In addition, two very large tropical storm events (1977 and 1983) signaled the return of tropical storm floods which had dominated the early record in the 1920s and 1930s, but then disappeared as an influence in the annual flood record.

The causes for the post-1965 shift in flood type, which has been observed on other regional rivers such as the Santa Cruz (Webb and Betancourt 1992), have been much debated. The most probable cause is a circulation response, through air-sea interactions, to changes in Pacific Ocean sea surface temperatures. El Niño years tend to be characterized by wetter-than-normal winter precipitation in the Southwest (Redmond and Koch 1991), and several studies on flooding in Arizona have pointed to an association between El Niño years and the occurrence of either large winter floods or late-season tropical storm floods (Webb and Betancourt 1992, Ely et al. 1994). It should be noted, however, that the Charleston record does not substantiate this linkage in all cases. Figure 7 compares El Niño years and the Niño-3 sea surface temperature index with the San Pedro annual flood series. There is some agreement between synoptic storm flood occurrences and the increased frequency of El Niño years since 1976 (especially in the 1990s), but the relationship is not consistent throughout the record. Several researchers have speculated on the possible role of the Pacific Decadal Oscillation (PDO) as a low-frequency influence on El Niño strength, such that positive phases of the PDO (shaded in fig. 7) enhance El Niño activity (see Gershunov and Barnett 1998, Gutzler et al. 2002). Seven of the nine tropical storm floods shown in figure 7 occurred during positive phases of the PDO, suggesting a possible low-frequency +PDO association, but winter synoptic flood occurrence does not appear to favor either phase of the PDO.

Spatial patterns. The magnitude and frequency of floods varies along longitudinal (upstream-downstream) river gradients. Figure 8 illustrates how selected San Pedro River floods linked to winter synoptic-scale precipitation, summer convective rainfall, and fall tropical storm-related precipitation each progressed downstream along the length of the river and were recorded sequentially at the main trunk stream gages in operation at the time of the flood. Overall, in the three types of floods, there is a tendency for peak discharges to increase with increasing drainage area in the upper basin above the Charleston gage, and then to decrease with increasing drainage area as the flood wave progresses downstream and into the lower basin. This is not surprising, because orographic effects cause more abundant precipitation in the

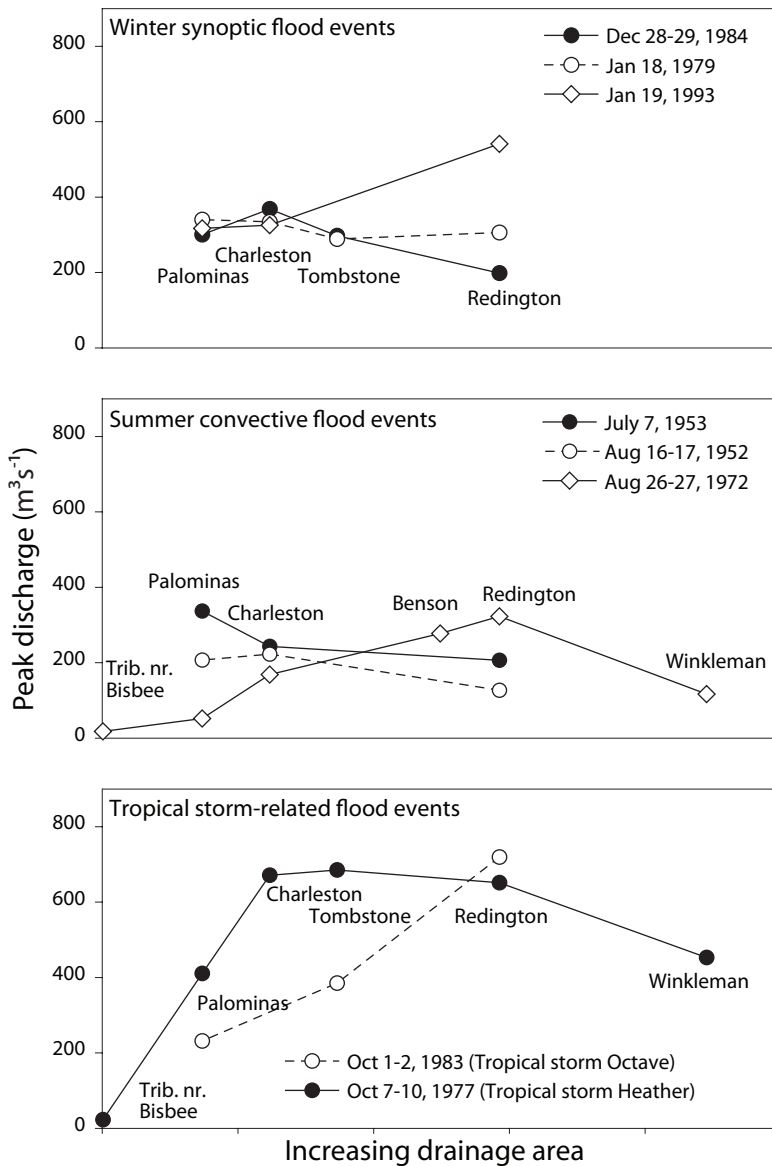


Fig. 16.8. Downstream progression of selected flood events of different types. (Values are instantaneous peak flows.)

mountains, and all of the large drainages from the high-elevation Huachuca Mountain range (except for the Babocomari) enter the San Pedro between the Palominas and Charleston gages. There have been exceptions to this trend, including the July 1953 convective event which *decreased* in size rapidly between Palominas and Charleston, suggesting a localized storm, and the 1983 flood associated with Tropical Storm Octave which *increased* dramatically as it traveled downstream and produced the flood of record at the lower basin stations near Mammoth and at Winkleman (table 1). Widespread heavy precipitation in the lower basin contributed to the downstream increase in 1983. Additionally, the higher drainage density in the lower basin can result in more rapid runoff and increased flood magnitude (see chap. 13).

Summary

The storm runoff or flood flow component of streamflow is much larger than the baseflow component, in terms of total volume, but is much more variable. Seasonally varying storm types cause the San Pedro streamflow and flood hydrographs to show a strong seasonal pattern. During the past century, about 90 percent of the annual maximum flood peaks occurred during July through October. Most of these were produced by summer monsoon convective thunderstorms which dominate in July and August. Floods associated with eastern Pacific tropical storms occurred most often in late summer and fall. Less than 10 percent of the annual floods occurred in December through March. Though average annual rainfall has not changed over time, the fluctuations in the annual distribution of that rainfall have influenced the flooding experienced by the San Pedro River. During the 1920s and 1930s, the largest annual floods were dominated by tropical storm events, and this gave way to dominance of the convective storm-driven annual floods until 1965, when the synoptic winter storms became dominant in the production of annual floods. Twice in the last 30 years, annual floods caused by tropical storms were among the largest floods on record in this basin.

Literature Cited in this Chapter

- Adams, D. K. and A. C. Comrie. 1997. The North American monsoon. Bulletin of the American Meteorological Society 78:2197-2213.
- Aldridge, B. N. and J. H. Eychaner. 1984. Floods of October 1977 in southern Arizona and March 1978 in central Arizona. U.S. Geological Survey Water-Supply Paper 2223.
- Aldridge, B. N. and T. A. Hales. 1984. Floods of November 1978 to March 1979 in Arizona and west-central New Mexico. U.S. Geological Survey Water-Supply Paper 2241.
- Bunn S.E., M.C. Thomas, S.K. Hamilton and S.J. Capon. 2006. Flow variability in dryland rivers: boom, bust and the bits in between. River Research and Applications 22: 179-186.
- Douglas M. W., R. A. Maddox and K. Howard. 1993. The Mexican monsoon. Journal of Climate 6:1665-1677.
- Ely, L. L., Y. Enzel and D.Cayan. 1994. Anomalous North Pacific atmospheric circulation and large winter floods in the southwestern United States. Journal of Climate 7:977-987.
- Gershunov, A. and T. P. Barnett. 1998. Interdecadal modulation of ENSO teleconnections. Bulletin of the American Meteorological Society 79: 2715-2725.
- Gutzler, D.S., D. M. Kann, and C. Thornbrugh. 2002. Modulation of ENSO-based long-lead outlooks of southwestern U.S. winter precipitation by the Pacific Decadal Oscillation. Weather and Forecasting 17: 1163-1172.
- Hirschboeck, K. K. 1987. Hydroclimatically-defined mixed distributions in partial duration flood series. In *Hydrologic Frequency Modeling*, ed. V.P. Singh. D. Reidel Publishing Company.
- Hirschboeck, K. K. 1988. Flood hydroclimatology. In Flood Geomorphology, eds. V.R. Baker, R.C. Kochel, and P.C. Patton. John Wiley & Sons.
- Hirschboeck, K. K. 1991. Climate and floods. In National Water Summary 1988-1989 -- Hydrologic Events and Floods and Droughts. U.S. Geological Survey Water-Supply Paper 2375: 67-88.
- House, P. K. and K. K. Hirschboeck. 1997. Hydroclimatological and paleohydrological context of extreme winter flooding in Arizona, 1993. In Storm-Induced Geological Hazards: Case Histories from the 1992-1993 Winter Storm in Southern California and Arizona, eds. Larson, R.A., and Slosson, J.E. Geological Society of America Reviews in Engineering Geology, v. XI, p. 1-24.
- Perry, C.A., Aldridge, B.N., and Ross, H.C. 2001. Summary of Significant Floods in the United States, Puerto Rico, and the Virgin Islands, 1970 Through 1989. U.S. Geological Survey Water-Supply Paper 2502.
- Redmond, K. T. and R. W. Koch. 1991. Surface climate and streamflow variability in the western United States and their relationship to large-scale circulation indices. Water Resources Research 27:2381-2399.
- Roeske, R. H., J. M. Garrett and J. H. Eychaner. 1989. Floods of October 1983 in southeastern Arizona. U.S. Geological Survey Water-Resources Investigations Report 85-4225-C.

Smith, W. 1986. The effects of eastern north Pacific tropical cyclones on the southwestern United States. NOAA Technical Memorandum NWS WR-197.

Tooth, S. and G.C. Nanson. 2000. Equilibrium and nonequilibrium conditions in dryland rivers. Physical Geography 21: 183-211.

Webb, R. H. and J.L. Betancourt. 1992. Climatic variability and flood frequency of the Santa Cruz River, Pima County, Arizona. U.S. Geological Survey Water-Supply Paper 2379.